A Quad-Band Low Power High Sensitive RF to DC Converter Circuit for RF Energy Harvesting Applications

Pavan Mehta* and Anveshkumar Nella

Abstract—In recent years, Radio Frequency Energy Harvesting (RFEH) has matured into a trustworthy and consistent method of obtaining ambient energy. For this energy to be utilized, it must be collected as efficiently over a broad range of frequencies as possible. In this regard, this article introduces a quad-band low-power, highly sensitive Radio Frequency (RF) to Direct Current (DC) signal converter circuit that operates at 1.5 GHz, 2.45 GHz, 3.6 GHz, and 5.5 GHz bands. The converter circuit is realized through single and dual-band converter circuit studies. These circuits comprise an impedance matching circuit, a voltage-doubler rectifier, a DC-pass filter with a resistive load of 5 kΩ, and a DC-DC voltage booster (LTC3108). The proposed quad-band converter circuit without a voltage booster gives a DC output voltage of 118 mV, 81 mV, 56 mV, and 24 mV at the four operational frequencies on a low input power of −25 dBm, respectively. A DC voltage of 3.3 V is obtained when the converter circuit is connected to a voltage booster. Maximum conversion efficiency achieved is 48% from four tones on a power input of −10 dBm. Circuit design steps, matching conditions, and performance parameters are presented using the Advanced Design System (ADS) and LTspice simulation tools.

1. INTRODUCTION

Technology improvements in wireless gadgets and devices have made our daily lives very easy [1, 2]. Most of these devices run on batteries, which limits their range, shortens their life, pollutes the environment, and makes it hard to replace them. As a result, energy harvesting is often proposed as potentially a means of obtaining power from nature [3]. Energy harvesting is the method for extracting energy from thermal energy, solar energy, wind energy, vibration stimulation, pressure gradients, and radio-frequency (RF) signals [4–8]. Compared to various harvesting methods, electromagnetic (EM) energy harvesting can create a sustainable energy source [9]. The use of electromagnetic energy harvesting is an environmentally friendly and cost-effective method of providing power for wireless devices, sensing networks, and portable Internet of Things (IoT) applications [10–12]. RF energy is a part of electromagnetic energy plentifully available in space due to the broadcast of different frequency bands in the environment and is governed by numerous standards. These standards include the Global System for Mobile Communication (2G), Universal Mobile Telecommunication System (3G), Long-Term Evolution (4G), 5G communication, Wireless Fidelity (Wi-Fi), and some modern applications used by societies, such as mobile telephony, intelligent environment monitoring, innovative medical applications, wireless Internet, satellite communication, radar systems, and broadcasting of radio and Television (TV) [13]. Figure 1 shows a block diagram architecture detailing the RFEH system. It includes (i) a receiving antenna (RF source) [14], for capturing RF power by far-field technique [15], and (ii) a matching network [16], to transmit the maximum power from the RF source to the voltage-doubler rectifier. This matching network has lumped elements (Resistor (R), Inductor (L), and Capacitor (C)) or distributed elements and maybe a combination of both types, (iii) a rectifier (voltage doubler +

* Corresponding author: Pavan Mehta (pawan71983@gmail.com).
The authors are with the School of EEE, VIT Bhopal University, Sehore, India.
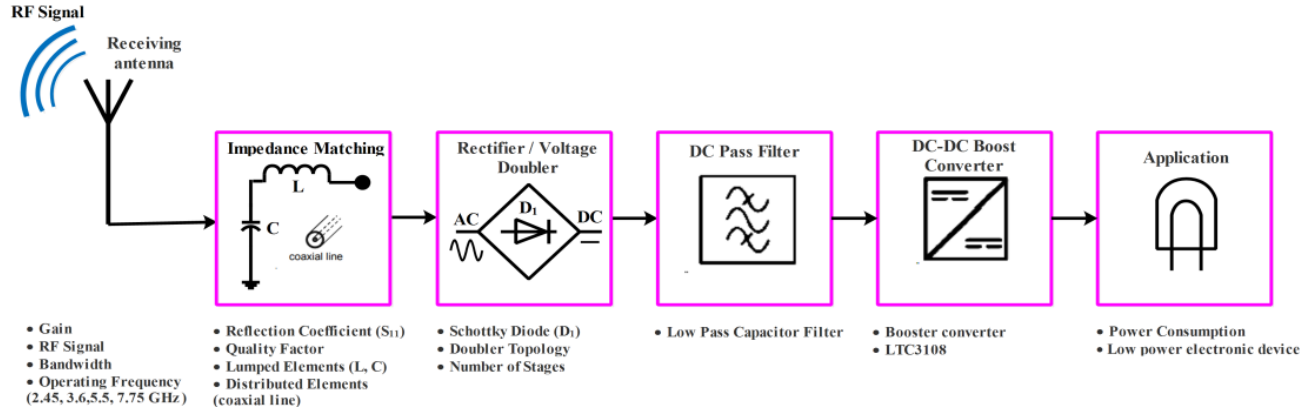
Figure 1. Block diagram of a radio-frequency energy-harvesting system.

rectification), to convert RF signal into DC and amplifies it by a zero-bias Schottky barrier diode in multistage topology, (iv) a DC pass filter circuit, consisting of a capacitor that effectively allows DC voltage while blocking higher-order harmonics of AC signal, and (v) a DC to DC step-up voltage converter [17], to boost up the small values of DC signal on the desired DC voltage for operating electronic devices.

In RFEH systems, the rectifier/RF-to-DC converter contributes a significant part in the transformation of RF to DC signals. From the concept of operating frequency, rectifiers are divided into four different categories, namely single-band [18–20], dual-band [21–23], quad-band or multiband [24–26], and broadband [27, 28]. Numerous rectifier configurations have been studied to evaluate the performance of a rectifier and its conversion efficiency (maximum utilizable power). In [18], the authors presented a highly compact printed rectenna designed at a frequency of 2.45 GHz. It offers a power conversion efficiency (PCE) of 17.7% at a power input of −20 dBm. A rectifier circuit based on a single shunt and series diode topology for converting RF-to-DC power at 3.5 GHz was presented by the authors in [20]. It achieved 67.16% peak conversion efficiency for a 5 dBm input power. The rectifier circuit presented for a single band in [18–20] is suitable for low-powered RFEH applications, but power conversion efficiency is low. The authors of [21] reported a dual-band rectifier that operates at 2.45 GHz and 5.5 GHz and is based on two full-wave rectifiers with Greinacher topologies for different frequencies. At an input power of 0 dBm, the rectifier achieved a maximum conversion efficiency of 36% and 8%. The authors in [22] proposed a dual-band rectifier based on the impedance transformer. This rectifier gives the conversion efficiency of 44.36% and 26.95% at 2.45 GHz and 5.8 GHz, respectively for −10 dBm input power. The concepts provided by the researchers in [21–23] are adequate for a low-powered RFEH module, but the conversion efficiency is subpar due to the excessive usage of filtering components in the selection of the frequency and diode nonlinearity. The authors proposed a quad-band rectifier using a lumped element-matching network for 0.9, 1.8, 2.1, and 2.4 GHz bands [24]. At −10 dBm input power, the rectifier achieved a maximum conversion efficiency of 42% at the two-tone signal. The authors of [25] described a quad-band RF circuit for the 0.9 GHz, 1.8 GHz, 2.1 GHz, and 2.45 GHz frequency bands based on a four-bandpass filter. The design recorded a peak conversion efficiency of 40% at a −10 dBm input power level for a four-tone signal. The authors of [27] proposed a compact broad-band rectenna for 3.27 GHz to 5.89 GHz frequency bands using the ADS tool. This rectenna design achieved a conversion efficiency of 39.18% at 0 dBm input power. A broad-band rectenna for RFEH devices was recommended in [28], using a Greinacher voltage doubler rectifier circuit for the 1.85 GHz to 6.85 GHz frequency band. This rectifier device achieved a maximum power conversion efficiency of 67.18% at 12 dBm input power. A high-powered RFEH module can be used with the designs described by the authors in [24–28] despite higher parasitic capacitance that reduces circuit performance. In the RFEH module, a multiband rectifier that harvests energy selectively from a few bands can be a better solution as a compromise between output power and conversion efficiency.

The primary goal of this endeavor is to develop and characterize a quad-band RF-to-DC converter circuit, which also includes a voltage boost converter (LTC3108). It proposes a quad-band converter

based on a lumped element circuit with enhanced PCE to harvest a low-powered RF signal up to a minimum value of -25 dBm. A lumped elements-based matching network matches the rectifier input impedance with the characteristic impedance of the source at 1.5 GHz, 2.45 GHz, 3.6 GHz, and 5.5 GHz along with a 5 kΩ resistive load. For optimum power conversion of RF-to-DC, a single voltage doubler rectifier with a quad-band impedance matching network and a voltage boost converter circuit (LTC3108) operated by an input DC signal ranging from 20 mV to 500 mV are considered. The proposed design can convert the low voltage of 20 mV to 3.3 V by using a DC-DC boost converter. ADS and LTspice tools are utilized for the proposed work's execution. The structure of this article is as follows. Section 2 explains the philosophy behind the design methodology of multi-band RF-to-DC signal converter circuits. Section 3 describes the design and analysis of the proposed quad-band RF-to-DC signal converter circuit. Section 4 discusses the integration of the DC-DC voltage booster circuit in association with the RF-to-DC signal converter and its experimental setup. Section 5 concludes this paper.

2. DESIGN METHODOLOGY OF MULTIBAND RF TO DC SIGNAL CONVERTER CIRCUITS

This section reports the design evolution of multiband RF-to-DC signal converter circuits using different types of converter topologies, like single-band and dual-bands. In the design of each topology, the main difference is the impedance-matching network. The rest of the circuitry is not affected by the number of operational bands. The lumped elements in the impedance-matching network increase as the number of operating bands increases. For instance, the single-band converter uses only two lumped elements while the dual-bands use four lumped elements, and the triple-bands use six lumped elements.

2.1. Single-Band RF to DC Signal Converter Circuit

Figure 2 illustrates an RF-to-DC signal converter circuit for converting RF energy acquired at 2.45 GHz. It consists of a single-band impedance-matching network, a rectifier, a DC pass filter, and a load resistor (R_L). The voltage doubler rectifier circuit uses a series-parallel combination of two Schottky diodes and a pair of 120 pF capacitors. The SMS7630-040 Skyworks Schottky diode is used for rectification since it has a breakdown voltage of $V_{br} = 2$ V, a low forward bias voltage of $V_{fwd} = 180$ mV, a low junction capacitance of $C_{jo} = 0.14$ pF, and a series resistance of $R_s = 20\,\Omega$ [29–33].

The performance of this rectifier is investigated using a co-simulation of harmonic balance and momentum at input-power levels ranging between -30 and 0 dBm. Figure 3(a) shows the graph between conversion efficiency and output vs. input power. The conversion efficiency and output voltage both gradually increase as input power increases. The conversion-efficiency ($\eta_{\mathrm{RF-DC}}$) is defined as a ratio between the output DC power transmitted on load (R_L) to the collected RF input power, and it is expressed by Equation (1) as follows:

$$\eta_{\mathrm{RF-DC}} = \frac{P_{\mathrm{DC}}}{P_{\mathrm{RF}}} \times 100\%, \tag{1}$$
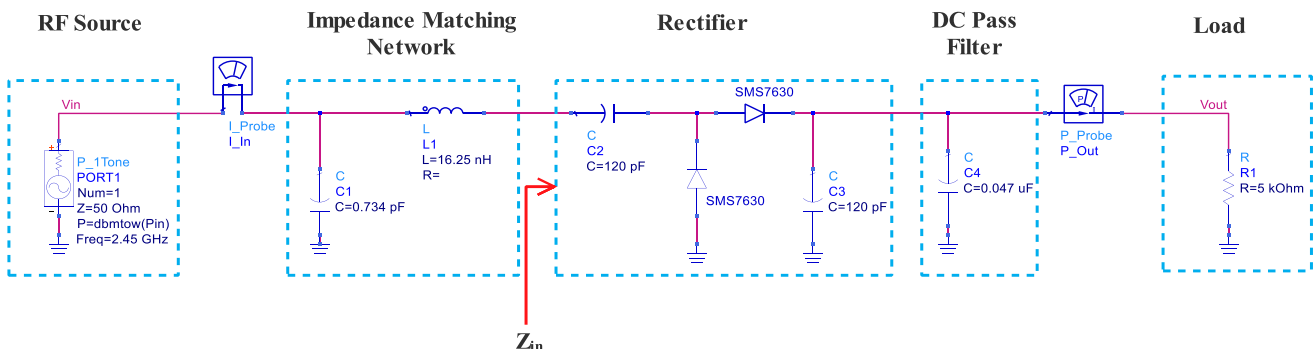

Figure 2. Electrical schematic design of a single band RF to DC signal converter circuit.

where P_{DC} represents the output DC power, and P_{RF} represents the input power of the converter. At $P_{\mathrm{in}} = -25\,\mathrm{dBm}$, a good match between the RF source and rectifier ($S_{11} \leq -40\,\mathrm{dB}$) is established, resulting in a conversion efficiency of 14.4% and DC voltage of 48 mV, respectively. Figure 3(b) illustrates the simulation results of the designed rectifying circuit at an input power of $-25\,\mathrm{dBm}$. It shows the rectifier's output with and without a filter circuit. A capacitor ($C_4 = 0.047\,\mathrm{\mu F}$) is used as a DC pass filter [35] after the rectifier circuit with the matching network. It is utilized to eliminate the fundamental-frequency signal and harmonics produced by the nonlinear behavior of diodes, as shown in the inset plot of Figure 3(b). An impedance-matching network is necessary for maximum power transfer between the RF source (antenna) and rectifier converter circuit [16].

At 2.45 GHz, the RF source impedance considered is $50\,\Omega$, whereas the rectifier impedance at an input power (P_{in}) of $-25\,\mathrm{dBm}$ is $30 - \mathrm{j}228\,\Omega$. As illustrated in Figure 2, conjugate-matching is performed utilizing an LC matching network comprising a capacitor (shunt) and an inductor (series). To have the
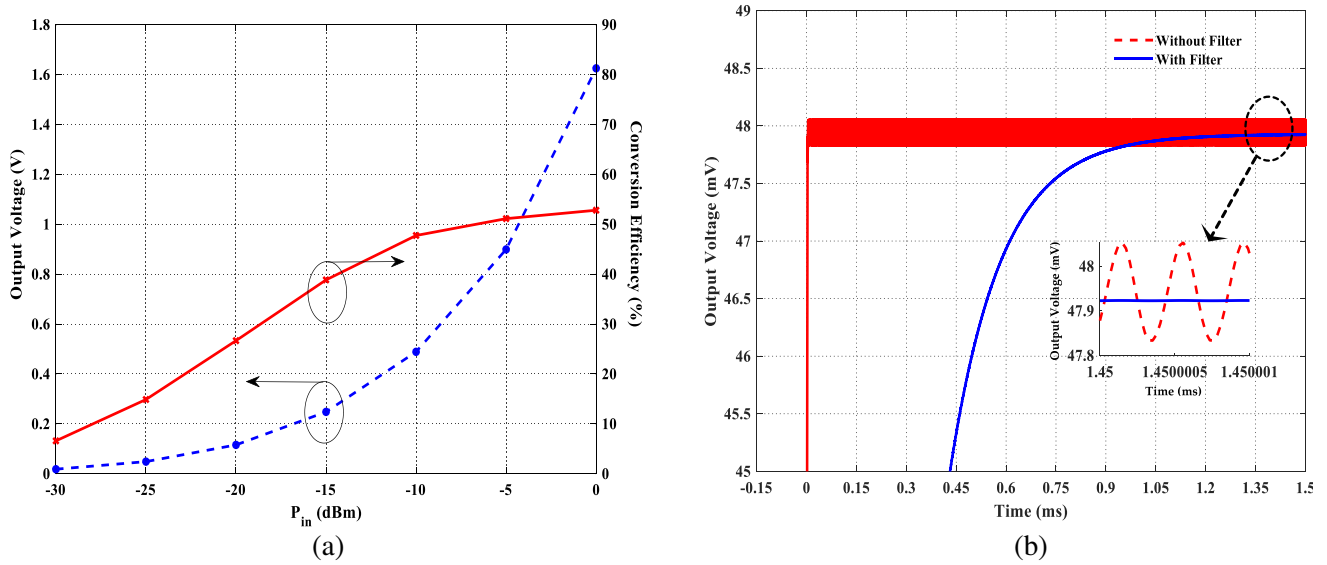

Figure 3. (a) Conversion-efficiency and DC voltage at frequency 2.45 GHz concerning input power (P_{in}) at $R_L = 5\,\mathrm{k}\Omega$; (b) The output voltage of the rectifier circuit with and without the DC pass filter.

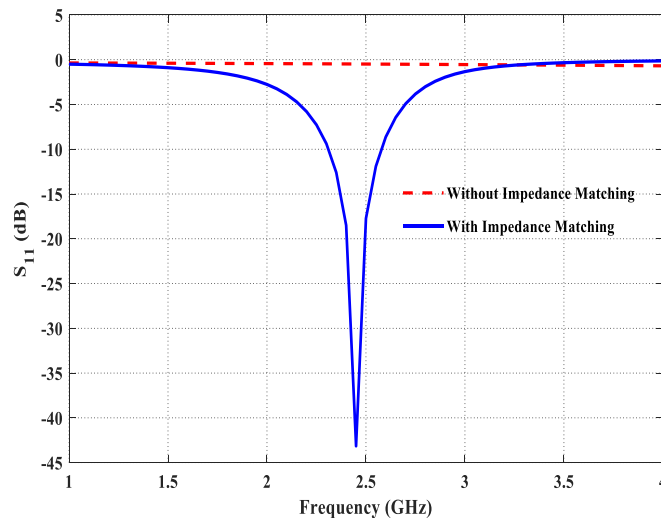**Figure 4.** Reflection coefficient of the rectifier circuit with and without impedance matching network.

impedance-matching at $2.45\,\mathrm{GHz}$, the extracted optimized values from ADS are $C_1 = 0.734\,\mathrm{pF}$ and $L_1 = 16.25\,\mathrm{nH}$, respectively. An equivalent impedance of the rectifier with a matching network is $(50 - \mathrm{j}0.692)\,\Omega$ which is quite near the RF source impedance. To analyze the rectifier's return-loss performance, considering an impedance matching circuit and without a matching circuit, a plot of the reflection coefficient (S_{11}) versus input frequency is shown in Figure 4. The return loss dramatically decreases at the matching frequency due to the impedance matching. The matching network has been constructed in a good match at an input power of $-25\,\mathrm{dBm}$.

2.2. Dual-Band RF to DC Signal Converter Circuit

A preferred dual-band RF-to-DC signal converter circuit layout is depicted in Figure 5. It also has a dual-band impedance-matching network, rectifier, DC pass filter, and load resistor (R_L). This circuit utilizes a dual-band matching network consisting of four lumped elements matching around $2.45\,\mathrm{GHz}$ and $5.5\,\mathrm{GHz}$ for input signals from an RF source.
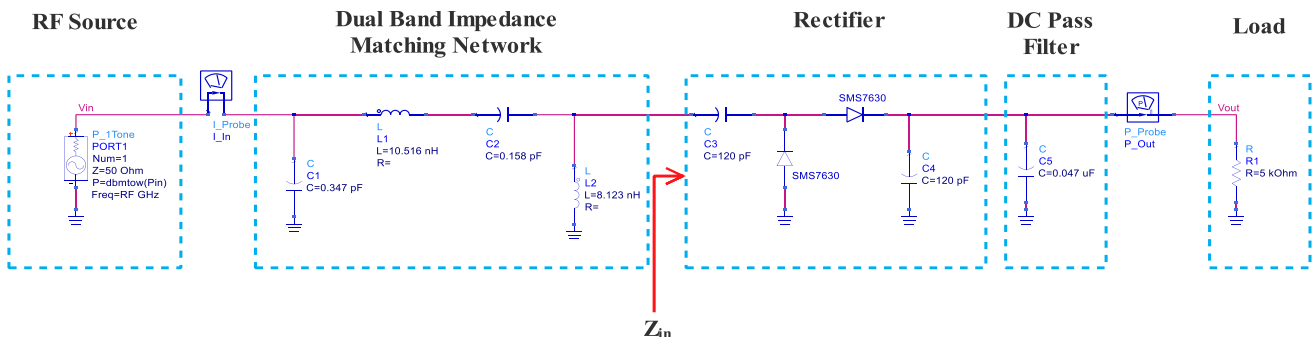

Figure 5. Electrical schematic design of a dual-band RF to DC signal converter circuit.

The conversion efficiency and DC output voltage are considered for the various input power levels. Figures 6(a) and (b) depict the simulated output DC voltage and conversion efficiency for applied signal frequencies at $R_L = 5\,\mathrm{k\Omega}$ load, respectively. The maximum conversion efficiency is 47% with an output voltage of $498\,\mathrm{mV}$ at $2.45\,\mathrm{GHz}$, and it is 27% with an output voltage of $366\,\mathrm{mV}$ at $5.5\,\mathrm{GHz}$ for $-10\,\mathrm{dBm}$ input power.
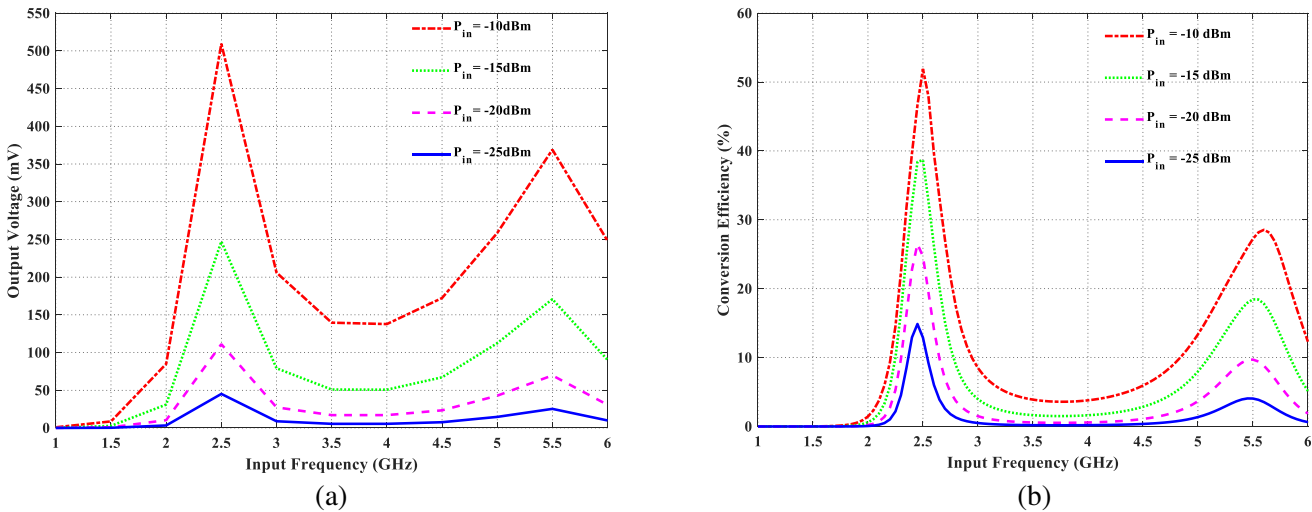

Figure 6. (a) Simulated output voltage; (b) Conversion-efficiency for different input power levels at $R_L = 5\,\mathrm{k\Omega}$.

The design of the circuit is mostly dependent on a matching circuit between the rectifier and RF source because the rectifier input impedance is nonlinear over a modest RF-input power range. Figure 7(a) shows the reflection coefficient characteristics from which it is depicted that when the input power changes from -25 dBm to -10 dBm, the reflection coefficient remains less than -10 dB. The -10 dB bandwidth of the converter has 100 MHz on the lower band centered at 2.45 GHz and 200 MHz on the upper band centered at 5.5 GHz, respectively. In an RF-to-DC converter, the shift towards higher frequencies as the RF input power increases while maintaining minimal S_{11} (reflection coefficient) can be attributed to nonlinear effects within the circuit components. As the RF power level rises, components such as diodes and lumped components may enter regions of nonlinearity in their voltage-current characteristics. In these regions, the response of the circuit becomes nonlinear, leading to harmonic generation and intermodulation distortion. These nonlinear effects introduce spectral components at higher frequencies, causing a shift towards higher values in the frequency domain. Consequently, at high frequencies, additional parasitic effects must be included in the component model.
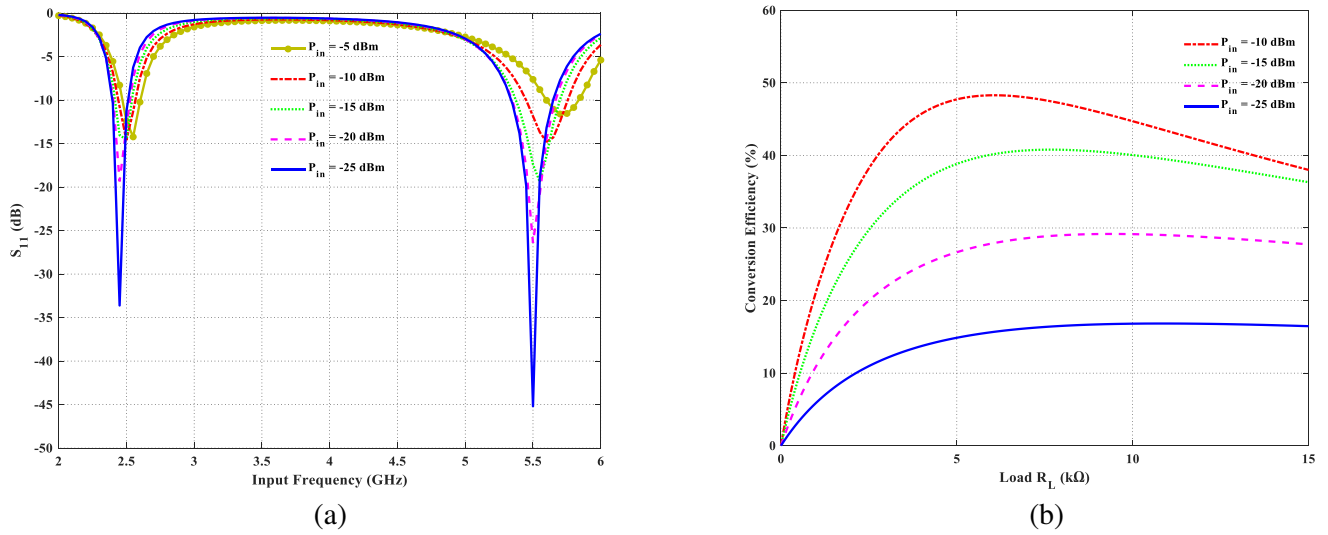

Figure 7. (a) Reflection coefficient of dual-band converter for different input power levels at $R_L = 5$ kΩ; (b) RF to DC signal converter circuit efficiency as a function of output load for different input power levels at 2.45 GHz.

The proposed rectifier covers the desired two bands for different input power levels of interest. The exact values of chip inductors and capacitors are normally a function of frequency. To reduce the influences, products with similar values but different series numbers can be used to replace the components with large values and designed for high frequencies (e.g., $L > 20$ nH, $C > 15$ pF, and $f > 1$ GHz) while multiple identical prototypes can be made to obtain better performance. This phenomenon can have practical implications, especially in RF energy harvesting applications, where maintaining optimal conversion efficiency and minimizing spectral interference is crucial. Figure 7(b) shows simulated conversion efficiency results versus optimum output load at different input power levels. For dual-band systems, simulation results show an optimum load value of 4.3 kΩ at 2.45 GHz. RF energy harvesting circuits employing loads ranging from 0 kΩ to 15 kΩ are applied in diverse fields. Lower-range loads (1–5 kΩ) power low-energy sensors for tasks like monitoring the environment and industrial processes. Medium-range loads (2–10 kΩ) can either extend the lifespan of batteries or eliminate their need in IoT devices. Loads within the 2–8 kΩ range are well-suited for wearable electronic devices, while loads of 5–15 kΩ are optimal for asset tracking in logistics. In sectors like smart packaging and building automation (with load values of 5–10 kΩ and 3–10 kΩ, respectively), RF energy harvesting enhances product security and boosts energy efficiency. Medical devices (1–8 kΩ) designed for remote monitoring profit from the efficient energy harvesting capabilities. The selection of the specific load value hinges on the unique power needs and efficiency criteria of each application.

3. PROPOSED QUAD BAND RF TO DC SIGNAL CONVERTER CIRCUIT

The proposed quad band converter has been realized using the concept of designing a single to multiband impedance matching network. As discussed in the previous section, the single band matching network requires two lumped elements. As the number of the operational bands is increased, the number of lumped elements is also increased by two for each additional band. Therefore, the proposed quad-band RF-to-DC converter circuit requires eight lumped elements to match the network as shown in Figure 8. The quad-band converter circuit impedance matching network is designed using a series-parallel combination of inductive and capacitive lumped elements. The operating bands around $1.5\,\mathrm{GHz}$, $2.45\,\mathrm{GHz}$, $3.6\,\mathrm{GHz}$, and $5.5\,\mathrm{GHz}$ for input RF signals are considered for the design of the proposed converter.
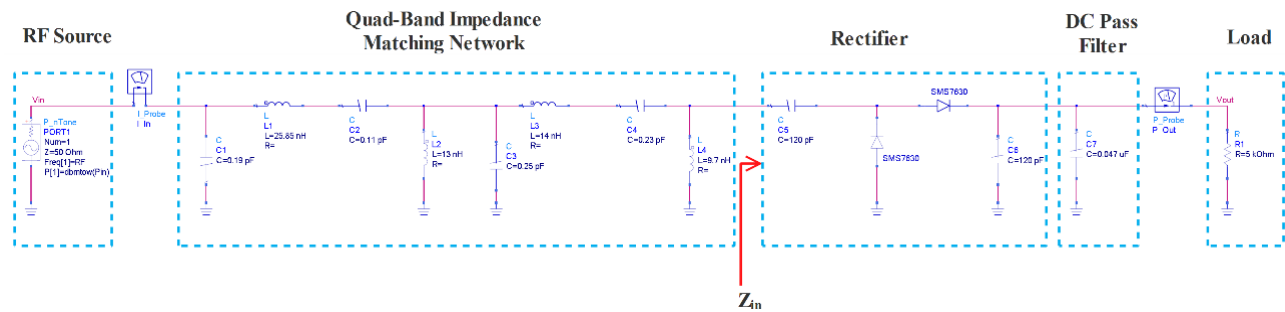

Figure 8. An electrical schematic of the proposed quad-band RF to DC converter.

3.1. Simulation Results and Discussion

The performance of this converter is investigated at the four operating frequencies with the usage of the ADS tool of Keysight. ADS's coexisting significant large signal S-parameter (LSSP) and harmonic balance (HB) simulation modules assess the rectifier's performance.

The proposed quad-band converter rectifier's simulated reflection coefficient (S_{11}) at each of the four operating frequencies is shown in Figure 9(a). The results show suitable impedance matching between the RF source and rectifier with a reflection coefficient of less than $-10\,\mathrm{dB}$ at all operating frequencies. Figure 9(b) shows the output voltage vs. input frequency graph when input power is set to $-25\,\mathrm{dBm}$ with a load of $5\,\mathrm{k\Omega}$. This converter circuit gives a DC output voltage of $118\,\mathrm{mV}$ at $1.5\,\mathrm{GHz}$, $81\,\mathrm{mV}$ at $2.45\,\mathrm{GHz}$, $56\,\mathrm{mV}$ at $3.6\,\mathrm{GHz}$, and $24\,\mathrm{mV}$ at $5.5\,\mathrm{GHz}$ across the load. Simulation results for

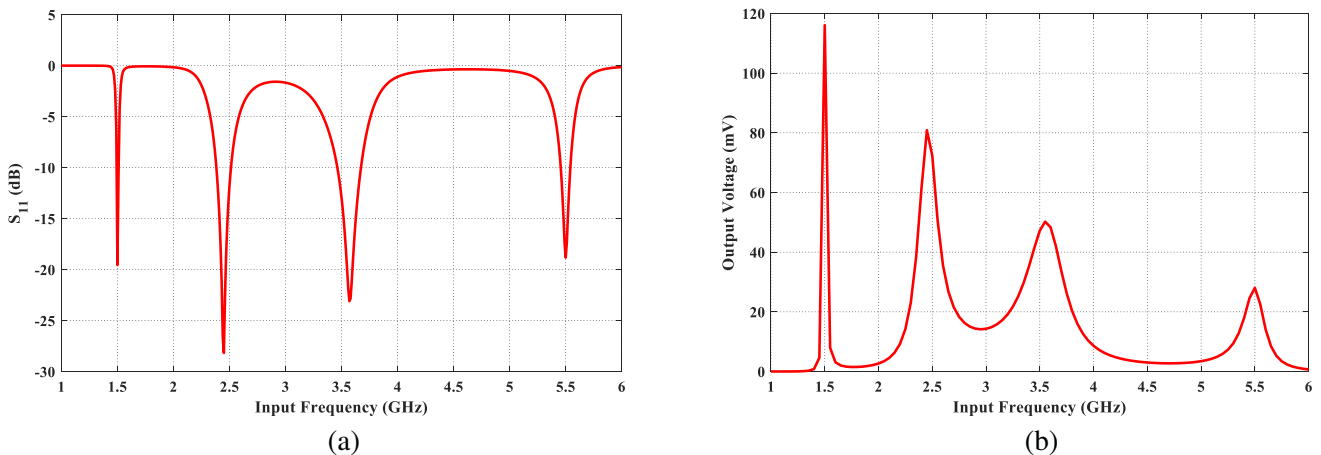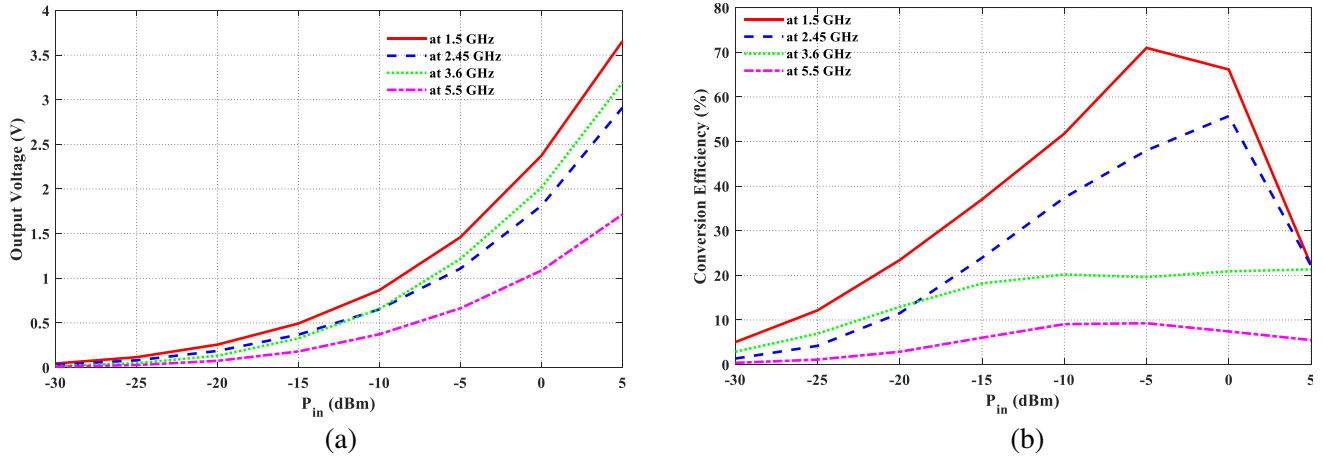**Figure 9.** (a) Simulated reflection coefficient (S_{11}); and (b) Output voltage of quad-band RF to DC converter at $P_{\mathrm{in}} = -25\,\mathrm{dBm}$.

Figure 10. (a) DC output voltage; and (b) Conversion-efficiency of quad-band converter circuit concerning input power (P_{in}) at $R_L = 5\,\text{k}\Omega$.

the converter's output voltage and RF-to-DC conversion efficiency as a function of RF input power are shown in Figures 10(a) and (b). From Figure 10(a), it is noted that the output voltage of the converter circuit at $5\,\text{k}\Omega$ load gradually increases as input power increases. Additionally, Equation (1) is used to compute the RF-to-DC conversion efficiency for each band of the rectifier [36]. From Figure 10(b), it can be depicted that the quad-band converter achieved peak simulated power conversion efficiencies of (12%, 7%, 4%, and 2%) for an input power of $-25\,\text{dBm}$ across all quad-band converter frequencies. When the input power level was $-10\,\text{dBm}$, the maximum simulated conversion efficiency was attained.

The corresponding values were 52% at $1.5\,\text{GHz}$, 38% at $2.45\,\text{GHz}$, 20% at $2.45\,\text{GHz}$, and 9% at $5.5\,\text{GHz}$. The performance of the proposed quad-band rectifier is also examined using the four signals, or signals from more than one tone. The simulation of the quad-band circuit is initially limited to one band. The first converter set is performed for the dual-tone signal, using two RF sources as input sources for the simulation. Two equal-power tones at $1.5\,\text{GHz}$ and $2.45\,\text{GHz}$ were sent into the rectifier. The corresponding input power from the two tones is used as the rectifier's input power. The simulation setups for three-tone ($1.5\,\text{GHz} + 2.45\,\text{GHz} + 3.6\,\text{GHz}$) and four-tone ($1.5\,\text{GHz} + 2.45\,\text{GHz} + 3.6\,\text{GHz} + 5.5\,\text{GHz}$) RF input power were repeated. When the multitone signals (two, three, and four) are applied to the rectifier, the output power will be changed. Equation (2) illustrates how to calculate the efficiency of a multitone signal [35]. The conversion efficiency ($\eta_{\text{RF}-\text{DC}}$) for four signals or multiple tones signals of the proposed rectifier is given by:

$$\eta_{\text{RF}-\text{DC}} = \frac{P_{\text{DC}}}{(P_{\text{RF1}} + P_{\text{RF2}} + P_{\text{RF3}} + P_{\text{RF4}})} \times 100\%, \tag{2}$$

where P_{DC} represents the output DC power, and P_{RF1}, P_{RF2}, P_{RF3}, and P_{RF4} represent the converter's input power at different tones. Figures 11(a) and (b) illustrate the simulated output DC voltage and RF-to-DC conversion efficiency of the proposed quad-band rectifier against input power for two, three, and four tones of RF input power, respectively. The output voltage plot, as shown in Figure 11(a), complies with the idea of multiband energy harvesting because it rises monotonically with the frequency band, especially at higher power levels. At an input power of $-25\,\text{dBm}$, the proposed quad-band rectifier could convert the four-tone RF signal into a DC signal with a peak PCE of 14.6%. Similarly, as shown in Figure 11(b), the proposed device achieved a maximum RF-to-DC conversion efficiency of 48% from the four-tone signal at a low input power level of $-10\,\text{dBm}$.

Table 1 compares the suggested quad-band rectifier with other relevant works from the literature. The proposed work harvests energy at many frequency bands compared to the results that have been published in [18–20, 22–25, 26–28] based on the number of frequency bands that have been used. The authors of [20, 22, 24, 25, 27] could get compactness at one and two working frequencies. Yet, this paper suggests a quad-band rectifier that delivers a higher improvement at low input power. Even
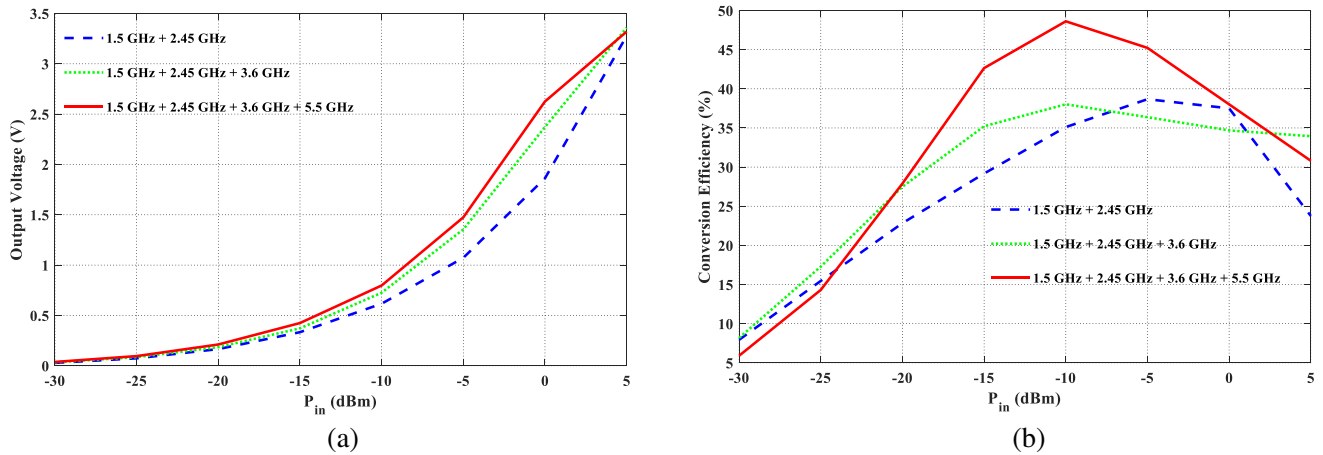
Figure 11. Simulated: (a) Output voltage; and (b) Conversion-efficiency of quad-band converter circuit concerning input power (P_{in}) at $R_L = 5\,\text{k}\Omega$ using one, two, three, and four signal tones.

Table 1. Comparison of proposed work with the literature.

Ref.	No. of bands	Freq. (GHz)	RF to DC converter Topology	Diode	P_{in} (dBm)	O/p Voltage (V)	R_L (kΩ)	Max. Efficiency
[18]	Single	2.45	Voltage doubler	HSMS2852	−20	0.091	4.7	17.7%
[20]	Single	3.5	Single series and shunt diode	HSMS2860	5	1.97	1.5	67.16%
[21]	Dual	2.45 and 5.5	Greinacher topology for different frequency	HSMS2852	0	-	12	36% and 8%
[23]	Dual	2.45 and 5	Full-wave voltage doubler rectifier	HSMS2860	15	3.2 / 1.8	1	35.4% / 20.9%
[25]	Quad	0.9, 1.8, 2.1 and 2.45	Single-stage voltage doubler	HSMS2852	−10	1.3	5	(40%: 4 tones)
[26]	Quad	0.75, 1.8, 2.4, and 5.8	Single-stage voltage doubler	HSMS2850	−10	1.7	11	(70%: 4-tones)
[27]	Broad	3.27 to 5.89	Greinacher voltage doubler	HSMS2860	0	3.08	1	39.18%
[28]	Broad	1.85 to 6.85	Greinacher voltage doubler	SMS7630	12	4.86	2.2	67.8%
This work	Quad	1.5, 2.45, 3.6, and 5.5	Single-stage voltage doubler	SMS7630-040	−10	0.867, 0.652, 0.630, and 0.373, and (0.790: 4-tones)	5	52%, 38%, 20%, and 9%, and (48%: 4-tones)

though the conversion efficiency of the proposed design is higher than that published in [21, 25, 26], it is still near that reported in [25] with low load. Compared to our suggested design, the rectifier used in [18, 21, 26] delivers less useful power for converting RF-to-DC. The improvement in conversion efficiency, output voltage, and the number of frequency bands gathered shows this work's importance

in this comparison. The level of the output voltage can also be boosted by adding up a DC-DC booster circuit. This boosted output voltage can be used to drive various low-power-enabled devices. However, these circuits' limitations in the practical implementation include bulkiness, low bandwidth, low radio power availability, low conversion efficiency, etc. For future work, we must deal with certain points like the improvement of power conversion efficiency and output voltage, enhancement of the operational frequency bandwidth, and matching requirements with the low power signals.

4. INTEGRATION OF LTC3108 POWER MANAGING CIRCUIT WITH PROPOSED QUAD-BAND RF TO DC SIGNAL CONVERTER CIRCUIT

A DC-DC booster circuit (LTC3108) is used, as shown in Figure 12, to increase the voltage obtained from the RF-to-DC signal converter circuit. The converter circuit output voltage is low at low input-power levels [31]. So, storing and utilizing energy is problematic. Hence, a DC-DC boosting circuit [34] can further enhance the output voltage. A highly integrated DC-DC converter, LTC3108 [35–37], is the ideal solution for harvesting and managing surplus power from low input voltage sources. The step-up topology operates from input voltages as low as $25\,\mathrm{mV}$ and gives an output voltage of up to $3.3\,\mathrm{V}$. In [37, 38], the input power levels of $-18\,\mathrm{dBm}$ and $-20\,\mathrm{dBm}$ achieve an output voltage of $32\,\mathrm{mV}$ to get $3.2\,\mathrm{V}$ from LTC3108. The proposed system's input power level is $-25\,\mathrm{dBm}$ for achieving the $3.3\,\mathrm{V}$ output. Figure 13 shows the result of LTC3108 connected to the proposed quad-band RF-to-DC signal converter circuit.
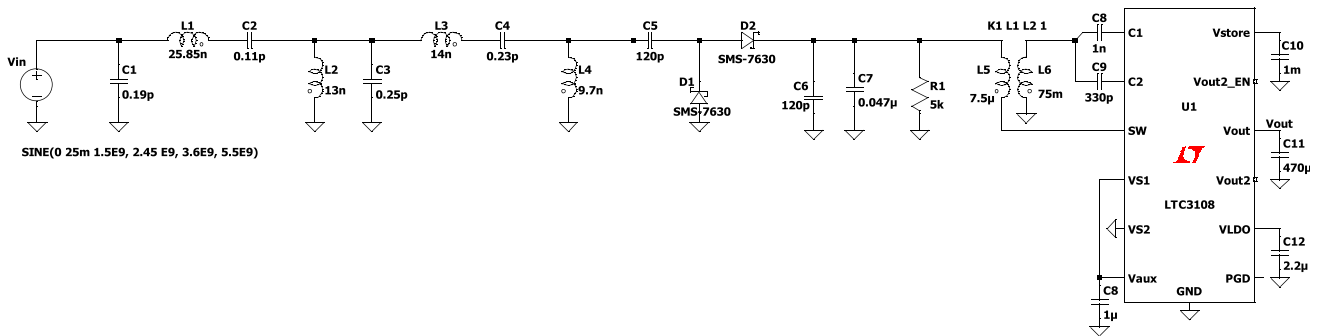

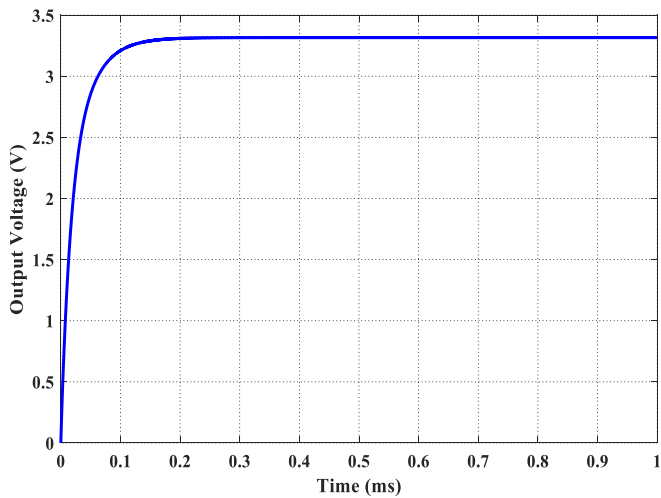**Figure 12.** LTC3108 connected to the proposed RF to DC signal converter circuit in LTspice.

Figure 13. The simulated output voltage of LTC3108.

4.1. Experimental Setup of the LTC3108 Boost Converter

The hardware module of the LTC3108 boost converter circuit is shown in Figure 14(a). This module consists of an LPR6235-752SML setup transformer, LTC3108, and several capacitors.

The output of this module is taken across an SMD capacitor of 2.2 µF. A 30 V, 3 A dual power DC supply from Scientific is used as an input source. An experiment is demonstrated to measure the performance of a DC-to-DC boost converter, as shown in Figure 14(b). It can be noted that for an input of 25 mV, the measured output voltage is around 2.49 V.
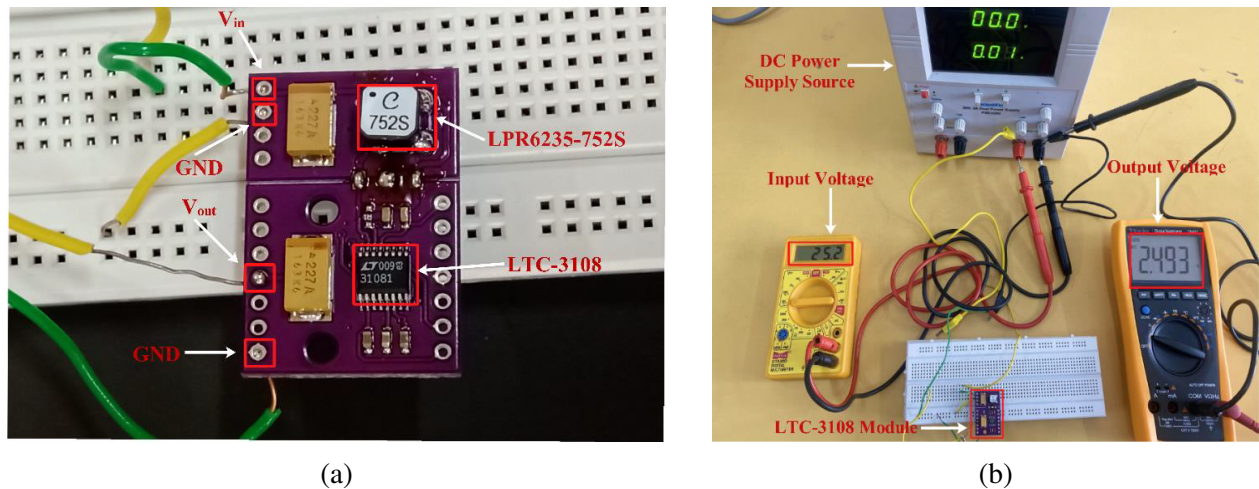

(a) (b)

Figure 14. (a) Experimental setup of LTC3108; (b) LTC3108 hardware module circuit.

5. CONCLUSION

In this study, the design of a quad-band RF to DC-signal converter circuit for energy-harvesting applications has been suggested. To match the rectifier's input impedance with an RF source at very low input power, a simple lumped element-based matching network is built. The simulated results show a good improvement in RF-to-DC power conversion efficiency. The proposed converter without a DC booster achieved PCEs of 52%, 38%, 20%, and 9% for an input power of −10 dBm at 1.5 GHz, 2.45 GHz, 3.6 GHz, and 5.5 GHz frequency bands. For an input power of −10 dBm, the converter achieved a peak PCE of 48% from the four-tone RF signal. With the LTC 3108 boost converter and a low −25 dBm input power, the suggested converter provides an output DC voltage of 3.3 V. Hence, the proposed converter circuit can be used in the application of low-power electronic devices and sensor networks in the Internet of Things.

STATEMENTS AND DECLARATION

Conflicts of Interest: The authors declare no conflict of interest.

REFERENCES

1. Paz, H. P., V. S. Silva, E. V. Cambero, H. X. Araújo, I. R. Casella, and C. E. Capovilla, "A survey on low power RF rectifiers efficiency for low-cost energy harvesting applications," *AEU-International Journal of Electronics and Communications*, Vol. 112, 52963, 2021.

2. Caselli, M., M. Ronchi, and A. Boni, "Power management circuits for low-power RF energy harvesters," *Journal of Low Power Electronics and Applications*, Vol. 10, 29, 2020.

3. Divakaran, S. K. and D. D. Krishna, "RF energy harvesting systems: An overview and design issues," *International Journal of RF and Microwave Computer-Aided Engineering*, Vol. 29, e21633, 2019.

4. Hesham, R., A. Soltan, and A. Madian, "Energy harvesting schemes for wearable devices," *AEU-International Journal of Electronics and Communications*, Vol. 138, 153888, 2021.

5. Gao, M., C. Su, J. Cong, F. Yang, Y. Wang, and P. Wang, "Harvesting thermoelectric energy from railway track," *Energy*, Vol. 180, 315–329, 2019.

6. Silva-Leon, J., A. Cioncolini, M. R. Nabawy, A. Revell, and A. Kennaugh, "Simultaneous wind and solar energy harvesting with inverted flags," *Applied Energy*, Vol. 239, 846–858, 2019.

7. Gaur, A., S. Tiwari, C. Kumar, and P. Maiti, "Polymer biowaste hybrid for enhanced piezoelectric energy harvesting," *ACS Applied Electronic Materials*, Vol. 2, 1426–1432, 2020.

8. Surender, D., T. Khan, F. A. Talukdar, A. De, Y. M. Antar, and A. P. Freundorfer, "Key components of rectenna system: A comprehensive survey," *IETE Journal of Research*, Vol. 68, 3379–3405, 2022.

9. Ibrahim, H. H., M. J. Singh, S. S. Al-Bawri, S. K. Ibrahim, M. T. Islam, A. Alzamil, and M. S. Islam, "Radio frequency energy harvesting technologies: A comprehensive review on designing, methodologies, and potential applications," *Sensors*, Vol. 22, 4144, 2022.

10. Ahmad, A., A. Ullah, C. Feng, M. Khan, S. Ashraf, M. Adnan, S. Nazir, and H. U. Khan, "Towards an improved energy efficient and end-to-end secure protocol for iot healthcare applications," *Security and Communication Networks*, 1–10, 2020.

11. Muncuk, U., K. Alemdar, J. D. Sarode, and K. R. Chowdhury, "Multiband ambient RF energy harvesting circuit design for enabling batteryless sensors and IoT," *IEEE Internet of Things Journal*, Vol. 5, 2700–2714, 2018.

12. Ashraf, S., T. Ahmed, and S. Saleem, "NRSM: Node redeployment shrewd mechanism for wireless sensor network," *Iran Journal of Computer Science*, Vol. 4, 171–183, 2021.

13. Khan, D., S. J. Oh, S. Yeo, Y. Ryu, S. In, R. E. Rad, I. Ali, Y. G. Pu, S. Yoo, M. Lee, and K. C. Hwang, "A solar/triboelectric/RF hybrid energy harvesting based high efficiency wireless power receiver," *IEEE Transactions on Power Electronics*, Vol. 36, 11148–11162, 2021.

14. Gaidhane, V. H., A. Mir, and V. Goyal, "Energy harvesting from far field RF signals," *International Journal of RF and Microwave Computer-Aided Engineering*, Vol. 29, e21612, 2019.

15. Boopathi, C. S., M. Sivaram, T. V. P. Sundararajan, R. Maheswar, P. Yupapin, and I. S. Amiri, "Bandenna for RF energy harvesting and flexible electronics," *Microsystem Technologies*, Vol. 27, 1857–1861, 2021.

16. Mohan, A. and S. Mondal, "An impedance matching strategy for micro-scale RF energy harvesting systems," *IEEE Transactions on Circuits and Systems II: Express Briefs*, Vol. 68, 1458–1462, 2020.

17. Churchill, K. K. P., G. Chong, H. Ramiah, M. Y. Ahmad, and J. Rajendran, "Low-voltage capacitive-based step-up DC-DC converters for RF energy harvesting system: A review," *IEEE Access*, Vol. 8, 186393–186407, 2020.

18. Koohestani, M., J. Tissier, and M. Latrach, "A miniaturized printed rectenna for wireless RF energy harvesting around 2.45 GHz," *AEU-International Journal of Electronics and Communications*, Vol. 127, 153478, 2020.

19. Shi, Y., J. Jing, Y. Fan, L. Yang, and M. Wang, "Design of a novel compact and efficient rectenna for WiFi energy harvesting," *Progress In Electromagnetics Research C*, Vol. 83, 57–70, 2018.

20. Meher, P., S. K. Mishra, and M. A. Halimi, "A low-profile compact broadband CP DRA for RF energy harvesting applications," *IETE Journal of Research*, 1–9, 2023.

21. Mattsson, M., C. I. Kolitsidas, and B. L. G. Jonsson, "Dual-band dual-polarized full-wave rectenna based on differential field sampling," *IEEE Antennas and Wireless Propagation Letters*, Vol. 17, 956–959, 2018.

22. El Mattar, S., A. Baghdad, and A. Ballouk, "A 2.45/5.8 GHz high-efficiency dual-band rectifier for low radio frequency input power," *International Journal of Electrical and Computer Engineering*, Vol. 12, 2169, 2022.

23. Dardeer, O. M., H. A. Elsadek, E. A. Abdallah, and H. M. Elhennawy, "A dual band circularly polarized rectenna for RF energy harvesting applications," *The Applied Computational Electromagnetics Society Journal (ACES)*, 1594–1600, 2019.

24. Agrawal, S., M. S. Parihar, and P. N. Kondekar, "A quad-band antenna for multiband radio frequency energy harvesting circuit," *AEU-International Journal of Electronics and Communications*, Vol. 85, 99–107, 2018.

25. Selim, K. K., S. Wu, D. A. Saleeb, and S. S. Ghoneim, "A quad-band RF circuit for enhancement of energy harvesting," *Electronics*, Vol. 10, 1160, 2021.

26. Keshavarz, R. and N. Shariati, "Highly sensitive and compact quad-band ambient RF energy harvester," *IEEE Transactions on Industrial Electronics*, Vol. 69, 3609–3621, 2021.

27. Behera, B. R., P. Srikanth, P. R. Meher, and S. K. Mishra, "A compact broadband circularly polarized printed monopole antenna using twin parasitic conducting strips and rectangular metasurface for RF energy harvesting application," *AEU-International Journal of Electronics and Communications*, Vol. 120, 153233, 2020.

28. Behera, B. R., P. R. Meher, and S. K. Mishra, "Metasurface superstrate inspired printed monopole antenna for RF energy harvesting application," *Progress In Electromagnetics Research C*, Vol. 110, 119–133, 2021.

29. SMS7630 SERIES, Skyworks Solutions, 2021. Available online: https://www.skyworksinc.com/-/media/SkyWorks/Documents/Products/201-300/Surface Mount Schottky Diodes 200041AG.pdf.

30. Mansour, M. M. and H. Kanaya, "Novel L-slot matching circuit integrated with circularly polarized rectenna for wireless energy harvesting," *Electronics*, Vol. 8, 651, 2019.

31. Mehta, P., A. Nella, and M. Rajagopal, "An RF energy harvesting system at 5.5 GHz for WLAN networks," *Proceedings of the 2021 IEEE Indian Conference on Antennas and Propagation (InCAP)*, 750–753, Jaipur, Rajasthan, India, December 2021.

32. Tafekirt, H., J. Pelegri-Sebastia, A. Bouajaj, and B. M. Reda, "A sensitive triple-band rectifier for energy harvesting applications," *IEEE Access*, Vol. 8, 73659–73664, 2020.

33. Muhammad, S., J. J. Tiang, S. K. Wong, A. Iqbal, A. Smida, and M. K. Azizi, "A compact dual-port multi-band rectifier circuit for RF energy harvesting," *Comput. Mater. Continua*, Vol. 68, 167–184, 2021.

34. Kim, J. and I. Kwon, "Design of a high-efficiency DC-DC Boost converter for RF energy harvesting IoT sensors," *Sensors*, Vol. 22, 10007, 2022.

35. LTC3108, Ultralow Voltage Step-Up Converter, and Power Manager. Analog Device. Available online: https://www.analog.com/media/en/technical-documentation/datasheets/LTC3108.pdf.

36. Chen, X., L. Huang, J. Xing, Z. Shi, and Z. Xie, "Energy harvesting system and circuits for ambient wifi energy harvesting," *Proceedings of the 2017 12th International Conference on Computer Science and Education (ICCSE)*, 769–772, Houston, TX, USA, August 22–25, 2017.

37. Pinto, D., A. Arun, S. Lenka, L. Colaco, S. Khanolkar, S. Betgeri, and A. Naik, "Design and performance evaluation of a wifi energy harvester for energizing low power devices," *Proceedings of the 2021 IEEE Region 10 Symposium (TENSYMP)*, 1–8, Jeju, Korea, August 23–25, 2021.

38. Di Marco, P., V. Stornelli, G. Ferri, L. Pantoli, and A. Leoni, "Dual band harvester architecture for autonomous remote sensors," *Sensors and Actuators A: Physical*, Vol. 247, 598–603, 2016.